

Article

Hydrogeochemistry of Shallow Groundwater in a Karst Aquifer System of Bijie City, Guizhou Province

Jianfei Yuan ¹ , Fen Xu ^{2,3,*}, Guoshi Deng ¹, Yeqi Tang ¹ and Pengyue Li ¹

¹ Chengdu Center of China Geological Survey, Chengdu 610081, China; jianfeiyuan@163.com (J.Y.); guoshi9456@126.com (G.D.); tyeqi@163.com (Y.T.); lpywudi02@163.com (P.L.)

² State Key Laboratory of Geohazard Prevention and Geoenvironment Protection, Chengdu University of Technology, Chengdu 610059, China

³ State Environmental Protection Key Laboratory of Synergetic Control and Joint Remediation for Soil & Water Pollution, Chengdu University of Technology, Chengdu 610059, China

* Correspondence: xufen1984@126.com; Tel.: +86-189-0821-3705

Received: 29 July 2017; Accepted: 16 August 2017; Published: 21 August 2017

Abstract: In this study, the major chemical compositions of 159 shallow groundwater samples incorporated saturation index (SI) and Principal Component Analysis (PCA) were employed to evaluate the mainly geochemical processes that control the hydrogeochemical evolution of groundwater in a typical karst area, Bijie city, Guizhou Province. The groundwater samples in this study area were dominated of HCO₃-Ca, HCO₃-Ca-Mg, and HCO₃-SO₄-Ca types. The PCA suggested that four principal components could explain 88.85% of the total variance of 10 parameters, indicating that the hydrogeochemical evolution of groundwater was mainly controlled by the dissolution/precipitation of carbonates, gypsum, and halite minerals, cation exchange, and anthropogenic activities. To be specific, the enrichment of Ca²⁺, Mg²⁺, HCO₃⁻ and SO₄²⁻ in groundwater were primarily affected by the dissolution of dolomite and gypsum minerals, and the role of calcite dissolution was relatively weaker because most groundwater samples were saturated with respect to calcite. Besides, cation exchange was another factor that may affect the concentration of Ca²⁺ and Mg²⁺ in groundwater, and the concentration of SO₄²⁻ can also be influenced by coal mining activity. In addition, the concentrations of Na⁺ and Cl⁻ in groundwater were likely influenced by the dissolution of halite, cation exchange, and human activities.

Keywords: major ions; PCA; water isotopes; karst aquifer; groundwater

1. Introduction

Southwest China is a typical karst area (covers about 620,000 km²) with a population of about 100 million. Karst groundwater is recognized as an indispensable water resource for drinking and irrigated agriculture in those regions [1]. The hydrogeochemical evolution of groundwater is typically affected by natural factors including the composition of rain water, geological structure and mineralogy of aquifer, and water-rock interaction along the flow paths [2–6]. In addition to natural processes, anthropogenic activities can also strongly influence the hydrogeochemical characteristic of groundwater [4,5,7–10]. In light of sustainable management of groundwater resources and scientifically challenging in complex karst settings, understanding the dominant processes that govern groundwater hydrogeochemical evolution is critically needed.

Previous studies have shown that the spatial variations of major ion concentrations and stable isotopic composition in groundwater are effectively used to determine groundwater recharge and flow path, source of solutes, interaction between groundwater and aquifer minerals, and the transport of

contaminant [1,2,4,6,9,11,12]. Recent studies, however, found that it is difficult to identify the primary process occurring in complex karst aquifers [13–16] with a large number of samples collected. A large number of studies have demonstrated that multivariate statistical methods such as PCA can usefully identify the geochemical processes taking place in aquifers, and distinguish anomalies between natural and anthropogenic influence on a variety of scales [17–28]. PCA has two obvious advantages, it is not only can effectively simplify the number of variables used without missing significant information, but also can conduce to the comprehensive classification of either variables or cases [13,16,29].

The study area is located in Bijie city, Guizhou Province, Southwest China, where karst groundwater occupies about 84% of the total groundwater resource. The main hydrogeological features of these karst aquifers have been investigated by the Chengdu Center of China Geological Survey in the year of 2013–2014 [30]. However, systematic studies to determine the hydrogeochemical evolution of groundwater within this region have not been performed. This study investigated the dominant processes controlling hydrogeochemical characteristics of karst groundwater in the study area by combining chemical analysis and PCA. The objectives of this study are (1) to investigate the spatial distribution of major ions in groundwater, (2) to identify the origin of groundwater, and (3) to determine the dominant geochemical processes and factors that controlling the hydrogeochemical characteristics of karst groundwater. The understanding of hydrogeochemical processes would reinforce the protection and sustainable utilization of water resources for the local government.

2. Geology and Hydrogeology Setting

2.1. Geographical Conditions

The study area is located between longitude $105^{\circ}15'–105^{\circ}30'$ E and latitude $27^{\circ}20'–27^{\circ}30'$ N in the northeast of Bijie city of Guizhou Province, Southwest China (Figure 1). It is about 210 km away from the Guiyang city, and covers an area of 450 km^2 . The climate of this area belongs to subtropical monsoon. The annual mean temperature is about $11.8\text{ }^{\circ}\text{C}$ from 1984 to 2013. The annual rainfall ranged from 615 to 1115 mm in the area in the past 30 years (1984–2013), with a mean value of 841 mm. The distribution of rainfall is uneven in this area, and about 50% of the annual rainfall occurs in June to August [30].

The topography of the study area gradually ascends from south and east to north and west, and the elevations range from 1220 to 2140 m above mean sea level. The surface rivers in Bijie are well-developed, which are the tributaries of Yangtze River. They could be divided into two main catchments (Wujiang River catchment and Chishui River catchment). The Chishui River catchment is located in the northern part of this region, mainly containing Zongji River, Cengtai River, Lengshuiyu River, and Mianyuhe River. The total drainage area of this catchment is about 1441.7 km^2 , accounting for 42% of the total area of Bijie city. The Baifu River is the major river of the Wujiang River catchment in the southwest part of the study area, with a drainage area of 2239.74 km^2 and a length of 110 km. The annual average runoff of this river is about $7.19 \times 10^9\text{ m}^3$ [30].

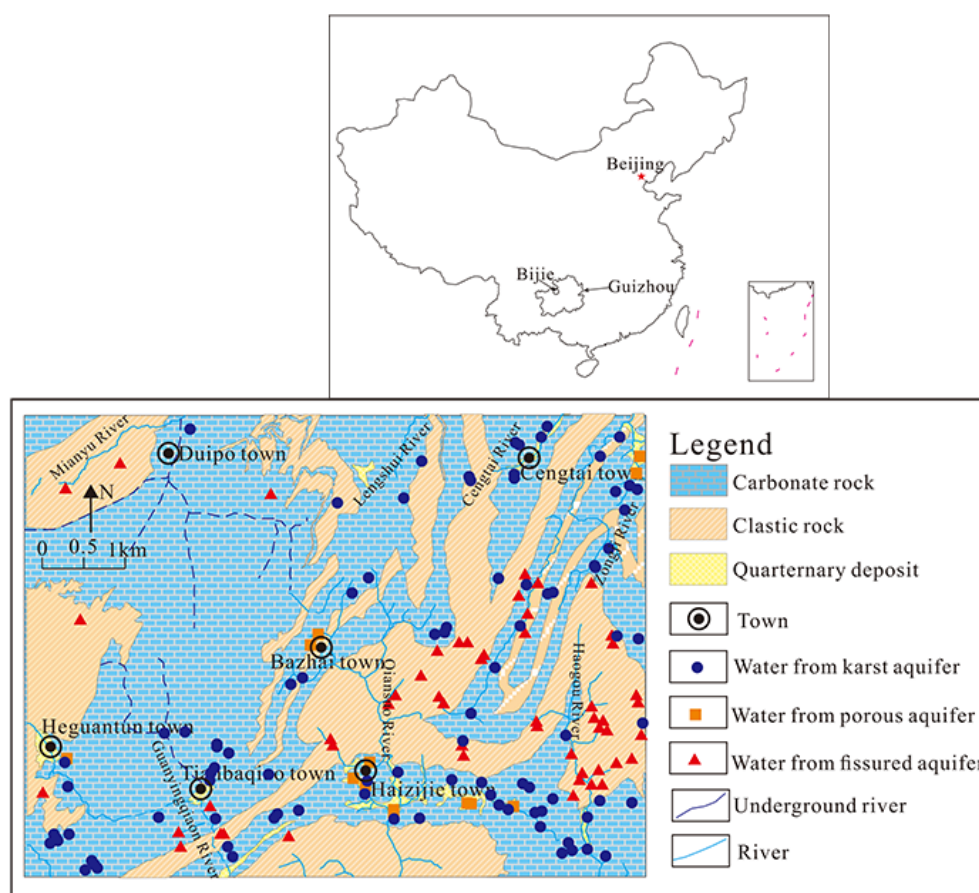


Figure 1. The geological setting map and sampling locations in the study area.

2.2. Geological and Hydrogeological Setting

The geological units from oldest to youngest in the study area are of Palaeozoic, Mesozoic and Quaternary deposits. Cambrian-Triassic layers comprise primarily of carbonate, which cover approximately 88.8% of the study area and identify as permeable rocks. Permian, Triassic and Jurassic clastic rocks, with S-rich coal containing strata, are made up of sandstone, mudstone, shale and argillaceous substrate. The unconsolidated Quaternary sediments rarely occur along a river or stream, and mainly consist of alluvial gravel, sand and clay [30]. A number of normal and inverse NNE and NE faults are observed in the study area, which affect the distribution of lithology, and control the groundwater flow.

Based on the occurrence and regional structure of groundwater in the study area, the groundwater in the study area could be classified into three groups, including water from the karst aquifer, porous aquifer, and fissured aquifer. Among them, water from the karst aquifer is the dominant water resources for drinking and irrigation in the study area, which accounts for 88.4% of groundwater. The karst aquifers are mainly constituted by Triassic limestone, dolomite, and dolomitic limestone, which has a widespread outcrop in the west of the study area. The sinkhole, karst cave, karst depression, and underground river are well-developed in this region. The spring discharges range from 0.02 to 175 L/s in these aquifers. Besides, water from fissured aquifer is also extensive distribution in Haizijie town and east of Bazhai town, and the spring flow varies from 0.01 to 1.42 L/s. Water from the porous aquifer is poorly observed in the study area, which primarily distributes in Haizijie town and river valley of Cengtai town, and it is seldom for domestic use. Generally, groundwater recharge in the study area is mainly via vertical infiltration of rain water, irrigation and lateral inflow from the mountains. With respect to the discharge of groundwater, the overall groundwater flow direction is from the

middle parts to south and to north using surface watershed as a boundary, and the groundwater is commonly discharged in the form of spring or spring groups along the river valley or the slope toe. In addition, the discharge of springs and underground flow shows a linear distribution along the riverbed [30].

3. Materials and Methods

3.1. Sampling and Analysis Methods

A set of 159 shallow groundwater samples were collected from springs, underground flow, and borehole during the summer (June to September) in 2013 for physicochemical analysis. The groundwater samples included water from the karst aquifer (N = 93), fissured aquifer (N = 52), and porous aquifer (N = 14). All samples were filtered using a 0.45 μm membrane filter and stored in new 500 mL polyethylene bottles, which had been washed with diluted nitric acid and rinsed with samples prior to sampling. Samples for cation analysis were acidified with ultrapure HNO_3 , the pH was less than 2 to prevent precipitation. While those for anion and stable isotope (H and O) analysis were not acidified. All water samples were preserved at 4 $^\circ\text{C}$ before laboratory measurement.

Temperature (T), pH, and the total dissolved solid (TDS) were measured in situ by portable Hanna meters (HI991301). Alkalinity (as HCO_3^-) was determined within 12 h using the titration method [31]. Cations (Ca^{2+} , Mg^{2+} , Na^+ , K^+) and anions (Cl^- , NO_3^- , and SO_4^{2-}) were determined in Chengdu Center of China Geology Survey by inductively coupled plasma atomic emission spectrometry (IRIS INTRE IIXSP, Thermo Fisher Scientific, Waltham, MA, USA), and ion chromatography (Dionex, DX-120, Thermo Fisher Scientific Inc., Waltham, MA, USA), respectively. The charge balances and uncertainties of the measured cation and anion concentrations were within $\pm 5\%$.

In this study, 20 groundwater samples were chosen to measure oxygen and hydrogen isotope by a mass spectrometer (MAT 253, Thermo Finnigan, Somerset, NJ, USA) at the Institute of Karst Geology, Chinese Academy of Geological Science. For the determination of $\delta^{18}\text{O}/^{16}\text{O}$ ratio, the CO_2 equilibration method was applied [32], and for the measurement of δD , the H_2 was generated by the Zn reduction method [33]. The stable O and D isotopic values can be expressed using usual notation of $\delta\text{‰}$ versus Vienna-Standard Mean Ocean Water (V-SMOW), where $\delta = (\text{R}_{\text{sample}}/\text{R}_{\text{SMOW}} - 1) \times 1000$, and $\text{R} = ^{18}\text{O}/^{16}\text{O}$ or D/H . The analytical precision for $\delta^{18}\text{O}$ and δD was 0.1 ‰ and 1 ‰ , respectively.

3.2. The Saturation Indices (SIs) of Minerals

The SI of mineral is an effective parameter to evaluate the degree of the chemical equilibrium between groundwater and aquifer minerals. It can be calculated as the following equation:

$$\text{SI} = \log \text{IAP}/\text{K} \quad (1)$$

where IAP is the ion activity product of the mineral, and K is the equilibrium constant of the mineral. Generally, the value of SI is greater than 0 meaning that the minerals were oversaturated with groundwater. Contrarily, the minerals were undersaturated with groundwater as the value of SI is less than 0. When the SI is equal to 0 indicates that the water-rock interaction reached an equilibrium status. The SIs of major minerals such as calcite (SI_{calcite}), dolomite (SI_{dolomite}), gypsum (SI_{gypsum}), SI_{aragonite}, SI_{halite} and anhydrite (SI_{anhydrite}) were evaluate by the geochemical program PHREEQC [34].

3.3. Principal Component Analysis (PCA)

Multivariate statistical analysis has been extensively applied to analyze the complex hydrogeochemical processes taking place in the aquifer [15,17,20,26,27,35]. In this study, the PCA was chosen to analyze the hydrochemical dataset. PCA is an efficient method to roughly identify the mechanisms with respect to groundwater chemical compositions [16,24]. In the PCA approach,

the chemical parameters such as Na^+ , K^+ , Ca^{2+} , Mg^{2+} , Cl^- , SO_4^{2-} , HCO_3^- , NO_3^- , TDS, and total hardness (TH) were firstly log transformed to improve symmetry, and z-standardization was used to reduce the variability [18,20,29]. T and pH were excluded from the analysis because there was a weak relationship between them and other parameters. The Kaiser Criterion was then employed to reveal the variability of groundwater samples, and the eigenvalues of principal components (PCs) > 1 was obtained. After that, the PCs loadings were calculated using a Varimax rotation, and finally the scoring weights of parameters were calculated [36]. PCA was performed by the software IBM SPSS statistics 19 (IBM SPSS statistics 19; IBM Corporation: Armonk, NY, USA) [37].

4. Results

4.1. Groundwater Chemistry

The statistical analysis of physicochemical parameters of groundwater samples were summarized in Table 1. The pH values of water from karst aquifer, fissured aquifer, and porous aquifer were mostly of neutral to slightly alkaline, and varied from 6.73 to 8.02, 6.40 to 7.80, and 7.10 to 7.90, respectively. The mean pH values of these three groups were 7.42 ± 0.22 , 7.27 ± 0.27 , and 7.32 ± 0.19 . TH and TDS are important parameters to evaluate the quality of drinking water [38]. In this study, the values of TH and TDS of these three groundwater groups ranged from 86.62 to 1519.78 mg/L and 51.67 to 1162.47 mg/L, 67.61 to 1018.30 mg/L and 34.42 to 789.93 mg/L, and 261.70 to 623.43 mg/L and 206.67 to 398.25 mg/L, respectively. Their average values were 378.00 ± 187.47 and 265.92 ± 134.82 mg/L, 301.04 ± 178.31 and 201.65 ± 127.76 mg/L, 406.74 ± 103.82 and 297.77 ± 58.22 mg/L, respectively. These results indicated that groundwater in this region is generally fresh water, and is weakly mineralized.

Table 1. Statistical analysis of the physicochemical parameters of groundwater samples from different aquifers.

Parameters	Water from karst Aquifer (N = 93)				Water from Fissured Aquifer (N = 52)				Water from Porous Aquifer (N = 14)			
	Min	Max	Mean	Stdev	Min	Max	Mean	Stdev	Min	Max	Mean	Stdev
T	12.5	19.1	15.1	1.3	13.2	28.4	15.2	2.8	13.9	16.9	15.1	0.9
pH	6.73	8.02	7.42	0.22	6.40	7.80	7.27	0.27	7.10	7.90	7.32	0.19
K^+	0.30	24.70	1.84	3.37	0.20	14.90	1.33	2.12	1.00	4.80	2.06	0.99
Na^+	0.00	35.50	2.61	4.17	0.60	15.70	3.25	2.38	1.10	6.40	3.10	1.70
Ca^{2+}	11.21	448.30	80.98	47.28	9.48	232.77	65.60	41.37	55.18	109.49	80.76	13.16
Mg^{2+}	1.05	60.64	15.47	14.03	2.09	50.19	9.19	9.40	7.32	46.53	23.34	12.66
Cl^-	0.95	32.16	6.18	4.50	1.89	14.66	4.60	3.19	5.20	21.28	11.18	5.82
SO_4^{2-}	10.00	920.00	72.79	110.13	8.00	580.00	75.75	91.25	14.00	80.00	47.20	21.16
HCO_3^-	4.97	432.48	208.20	68.35	9.94	298.26	136.90	67.59	173.99	382.77	278.02	59.03
NO_3^-	0.00	104.00	23.14	19.86	0.00	50.00	16.29	12.31	6.00	48.00	17.50	11.26
TDS	86.62	1519.78	378.00	187.47	67.61	1018.30	301.04	178.31	261.70	623.43	406.74	103.82
TH	51.67	1162.47	265.92	134.82	34.42	789.93	201.65	127.76	206.67	398.25	297.77	58.22
$\text{CO}_2(\text{g})$	-3.26	-1.47	-2.19	0.29	-3.14	-1.57	-2.26	0.29	-2.69	-1.60	-1.96	0.26
$\text{SI}_{\text{calcite}}$	-2.89	0.50	-0.06	0.38	-2.39	0.50	-0.49	0.56	-0.20	0.32	0.03	0.14
$\text{SI}_{\text{dolomite}}$	-5.87	0.70	-0.77	0.84	-5.10	0.10	-1.67	1.15	-1.20	0.33	-0.33	0.45
$\text{SI}_{\text{gypsum}}$	-2.53	-0.22	-1.83	0.38	-2.69	-0.59	-1.88	0.44	-2.44	-1.70	-1.92	0.26
$\text{SI}_{\text{anhydrite}}$	-3.12	-1.41	-2.24	0.38	-3.08	-1.00	-2.29	0.44	-2.87	-2.09	-2.33	0.26
$\text{SI}_{\text{aragonite}}$	-0.88	0.40	-0.21	0.38	-2.54	0.49	-0.64	0.56	-0.35	0.17	-0.12	0.14
$\text{SI}_{\text{halite}}$	-10.71	-7.87	-9.60	0.53	-10.20	-8.70	-9.51	0.35	-9.79	-8.51	-9.14	0.45

The physicochemical parameters are in mg/L except pH, T in $^{\circ}\text{C}$, TDS is the total dissolved solid, TH is total hardness as CaCO_3 .

The concentrations of K^+ and Na^+ in groundwater were much lower than that of Ca^{2+} and Mg^{2+} . The average concentrations of K^+ were 1.84 ± 3.37 , 1.33 ± 2.12 , and 2.06 ± 0.99 mg/L in water from karst aquifer, fissured aquifer, and porous aquifer, respectively. And the mean contents of Na^+ in these groups were 2.61 ± 4.17 , 3.25 ± 2.38 , and 3.10 ± 1.70 mg/L, respectively. The average concentrations of Ca^{2+} and Mg^{2+} in these three groundwater groups were 80.98 ± 47.28 and 15.47 ± 14.03 mg/L, 65.60 ± 41.37 and 9.19 ± 9.40 mg/L, 80.76 ± 13.16 and 23.34 ± 12.66 mg/L, respectively. The relative abundances of major cations in these three groundwater groups were mostly in a descending order:

$\text{Ca}^{2+} > \text{Mg}^{2+} > \text{Na}^+ > \text{K}^+$ (in meq/L). With respect to major anions such as HCO_3^- , SO_4^{2-} , and Cl^- , the mean concentrations of these chemical parameters were 208.20 ± 68.35 , 72.79 ± 110.13 and 6.18 ± 4.50 mg/L in water from karst aquifer, 136.90 ± 67.59 , 75.75 ± 91.25 and 4.60 ± 3.19 mg/L in water from fissured aquifer, and 278.02 ± 59.03 mg/L, 47.20 ± 21.16 and 11.18 ± 5.82 mg/L in water from porous aquifer. The relative abundances of these major anions were as follows: $\text{HCO}_3^- > \text{SO}_4^{2-} > \text{Cl}^-$ (in meq/L). These results suggested that Ca^{2+} , Mg^{2+} , HCO_3^- and SO_4^{2-} were the dominant ions in this region. For the ions Ca^{2+} , Mg^{2+} , and HCO_3^- , the mean values of them in both water from the karst aquifer and porous aquifer were higher than that of water from the fissured aquifer. For SO_4^{2-} , the average concentration in water from the porous aquifer was lower than that in water from both the karst aquifer and fissured aquifer.

The concentrations of the seven major ions (K^+ , Na^+ , Ca^{2+} , Mg^{2+} , HCO_3^- , SO_4^{2-} , and Cl^-) were plotted on a Piper diagram to evaluate the hydrochemical types of groundwater. It has found that the hydrochemical types of water from karst aquifer were complex, and the predominant types were $\text{HCO}_3\text{-Ca}$, $\text{HCO}_3\text{-Ca-Mg}$, and $\text{HCO}_3\text{-SO}_4\text{-Ca}$ (Figure 2). $\text{HCO}_3\text{-SO}_4\text{-Ca}$ and $\text{HCO}_3\text{-Ca}$ were the major hydrochemical types for water from fissured aquifer, accounting for 63% and 23% of the total samples ($N = 52$), respectively. The water from the porous aquifer mostly belonged to $\text{HCO}_3\text{-Ca}$ and $\text{HCO}_3\text{-Ca-Mg}$ types. The similar chemical composition of three different groundwater groups suggested their similar evolution mechanisms or frequent interaction between water from the karst aquifer and other water types (water from the fissured aquifer and porous aquifer).

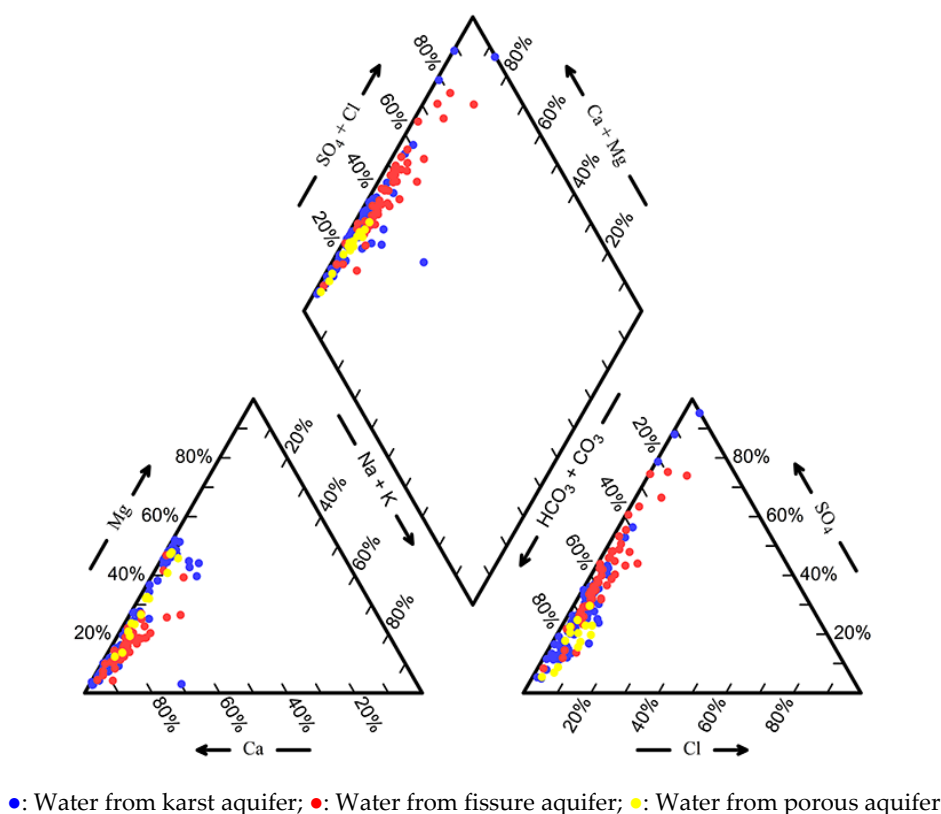


Figure 2. Piper diagram of groundwater samples in the study area.

Nitrate is a common contaminant in groundwater in China [38]. In the study area, the concentration of NO_3^- in water from karst aquifer, fissured aquifer, and porous aquifer ranged from 0.00 to 104.00, 0.00 to 50.00, and 6.00 to 48.00 mg/L, with an average of 24.14 ± 19.86 , 16.29 ± 12.31 , and 17.50 ± 11.26 mg/L, respectively. In addition, accounts for 6.3% of the total groundwater samples

were higher than the drinking water standard of the WHO for NO_3^- (50 mg/L) (WHO, 2008) [39], and these groundwater samples were mainly located at or near a residential area.

The SI for calcite, dolomite, gypsum, anhydrite, aragonite, and halite of three different groundwater groups were presented in Table 1. The SI values of gypsum, anhydrite, and halite for all groundwater are less than 0, suggesting that gypsum, anhydrite, and halite were under-saturated, and they could be feasibly dissolved along the flow path of groundwater. The average SI values of calcite and dolomite for water from the karst aquifer, fissured aquifer, and porous aquifer were -0.06 ± 0.38 and -0.77 ± 0.84 , -0.49 ± 0.56 and -1.67 ± 1.15 , and 0.03 ± 0.14 and -0.33 ± 0.45 , respectively. In water from both the karst aquifer and porous aquifer, most of them were nearly saturated or super-saturated with respect to calcite, and there were no obvious correlations between TDS values and SI for calcite (Figure 3a), indicating that calcite do not keep dissolving along the flow path. In contrast, the SI values of most of the water from karst aquifer and porous aquifer were less than 0, and they exhibit positive correlations with TDS, which suggested that most of them were under-saturated with respect to dolomite, and dolomite will continue to dissolve along the flow path (Figure 3b). For water from fissured aquifer, there were obvious positive correlations between TDS values and SI for both calcite and dolomite (Figure 3), indicating that both calcite and dolomite dissolve into water from the fissured aquifer along the flow path and increase the contents of TDS.

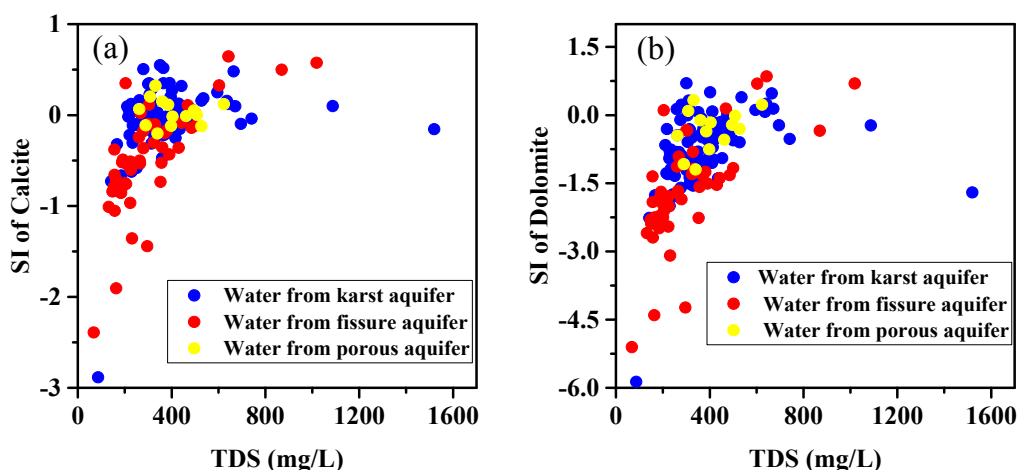


Figure 3. Correlation between total dissolved solid (TDS) and saturation index (SI) of (a) calcite and (b) dolomite in the study area.

4.2. Deuterium and Oxygen Isotopes

Environmental isotopes, such as oxygen and hydrogen isotope, were usually used as a natural tracer to identify the origin of groundwater [1,2,11,40]. In this study, δD for groundwater varied from -67.0‰ to -52.5‰ , with an average of -59.3‰ . And the values of $\delta^{18}\text{O}$ in groundwater ranged from -9.81‰ to -8.12‰ , with a mean of -8.97‰ . The relationship of δD to $\delta^{18}\text{O}$ was plotted in Figure 4. All groundwater was distributed around the Local Meteoric Water Line (LMWL) (dash line in Figure 4: $\delta\text{D} = 8.59\delta^{18}\text{O} + 17.7$) [41], and far away from the Global Meteoric Water Line (GMWL) (solid line in Figure 4: $\delta\text{D} = 8\delta^{18}\text{O} + 10$) [42] (Figure 4). This indicated that groundwater in this region originated from local meteoric water. Moreover, there was no obvious isotope shift in $\delta^{18}\text{O}$ for groundwater, which suggested a rapid runoff and short residence time of groundwater in the study area.

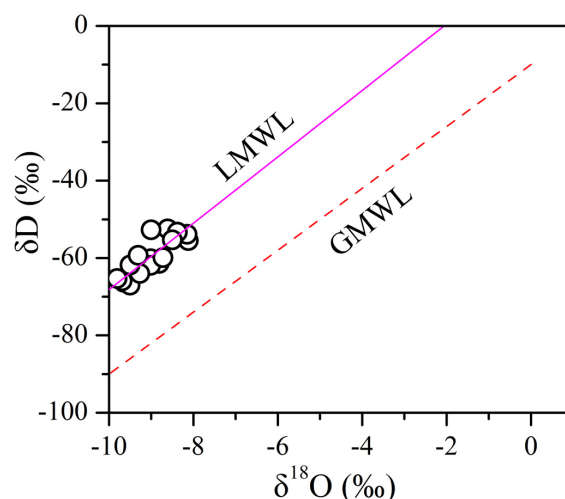


Figure 4. Oxygen and hydrogen isotope of groundwater samples associated with Global Meteoric Water Line (GMWL) and Local Meteoric Water (LMW) in the study area.

4.3. PCA of Hydrochemistry

The correlations among the 10 variables were presented in Table 2. It showed that most parameters have strong correlation with more than one other parameter. PCA results indicated that four PCs with eigenvalues greater than 1 (PC1, PC2, PC3, and PC4) could explain 88.85% of the total data variability (Table 3). PC1, PC2, PC3 and PC4 accounted for 49.34%, 14.88%, 13.31%, and 11.32% of the total variance, respectively. PC1 has significant positive loadings of Ca^{2+} , SO_4^{2-} , TH and TDS, with loadings of 0.934, 0.803, 0.847, and 0.816, respectively. This indicated that PC1 represents the dissolution/precipitation of carbonate and sulfate minerals. PC2 was mainly associated with significant loadings of K^+ , Mg^{2+} , and HCO_3^- , which represented chemical processes between infiltrated water and dolostone and clastic rocks (K-feldspar and mica). PC3 was related to Cl^- and NO_3^- . Nitrate is a common groundwater pollutant, which mainly comes from agricultural, domestic sewages and livestock excreta [43,44]. Therefore, PC3 represented the influence of anthropogenic activities. PC4 was highly loaded by Na^+ . The enrichment of Na^+ in groundwater mainly stems from the dissolution of halite, cation exchange between Na^+ and Mg^{2+} or Ca^{2+} , and anthropogenic activities. On the whole, PCA revealed that the chemical processes occurring in the groundwater aquifer was fairly complex, and the hydrogeochemical characteristics of groundwater were affected by dissolution/precipitation of minerals (such as carbonates, gypsum, and halite minerals), cation exchange, and anthropogenic activities. It is worth noticing that the first two PCs (PC1 and PC2) accounted for 64.22% of the variance, indicating that water-rock interactions (dissolution/precipitation of minerals) were the major factor influencing the hydrogeochemical characteristics of groundwater in the study area.

Table 2. Pearson correlation matrix of groundwater samples in the study area.

Parameters	K^+	Na^+	Ca^{2+}	Mg^{2+}	Cl^-	SO_4^{2-}	HCO_3^-	NO_3^-	TH	TDS
K^+	1.00									
Na^+	0.46	1.00								
Ca^{2+}	0.27	0.17	1.00							
Mg^{2+}	0.53	0.12	0.25	1.00						
Cl^-	0.62	0.39	0.41	0.25	1.00					
SO_4^{2-}	0.24	0.40	0.66	0.23	0.16	1.00				
HCO_3^-	0.38	-0.01	0.72	0.58	0.41	0.19	1.00			
NO_3^-	0.14	-0.01	0.26	-0.05	0.54	-0.05	0.20	1.00		
TH	0.45	0.14	0.90	0.63	0.43	0.61	0.84	0.17	1.00	
TDS	0.48	0.21	0.84	0.59	0.45	0.62	0.77	0.21	0.94	1.00

Bold refers to chemical parameters with a very significant correlation greater than 0.5.

Table 3. Loadings for varimax rotated factor matrix of chemical datasheet (significant loadings are marked in bold).

Variables	Principal Components			
	PC1	PC2	PC3	PC4
Ca ²⁺	0.934	0.128	0.245	0.036
SO ₄ ²⁻	0.803	−0.094	−0.187	0.447
TH	0.847	0.499	0.147	0.029
TDS	0.816	0.469	0.170	0.107
Mg ²⁺	0.232	0.884	−0.110	0.072
K ⁺	0.083	0.656	0.261	0.575
HCO ₃ ⁻	0.590	0.639	0.262	−0.212
NO ₃ ⁻	0.108	−0.092	0.913	−0.073
Cl ⁻	0.174	0.319	0.748	0.412
Na ⁺	0.110	0.030	0.042	0.915
Eigenvalue	4.934	1.488	1.331	1.132
Explained variance (%)	49.34	14.88	13.31	11.32
Cumulative % of variance	49.34	64.22	77.53	88.85

5. Discussion

PCA indicated that the hydrogeochemical characteristics of groundwater are typically controlled by water-rock interaction (carbonate, evaporates, and clastic rocks dissolution and/or precipitation), cation exchange, and anthropogenic activities such as the using of chemical fertilizer, livestock excreta, domestic sewages, and coal mining activities [45,46]. In this section, PCA results incorporated ion concentrations, and stable isotopes (oxygen and hydrogen isotope) were used to identify the dominant processes controlling hydrogeochemical characteristics of groundwater in the study area.

5.1. Rock Weathering

Gibbs diagrams are an effective tool to identify the major natural geochemical processes (such as atmospheric precipitation, rock weathering, and evaporation precipitation) controlling the hydrogeochemical characteristics of groundwater in the aquifer. The diagrams describe the weight ratios of Na⁺/(Na⁺ + Ca²⁺) and Cl⁻/(Cl⁻ + HCO₃⁻) against TDS [47]. As shown in Figure 5, most groundwater samples (except samples GW11 and GW54) were located in the rock weathering zone. In addition, carbonates (calcite, dolomite, and gypsiferous layer) and clastic rocks (K-feldspar and mica) are widespread in the study area. Therefore, dissolution /precipitation of carbonates and clastic rocks could be the crucial processes influencing the evolution of hydrogeochemical characteristics of groundwater in the study area. However, unlike the other groundwater samples, sample GW11 and GW54 were located between rock weathering and atmospheric precipitation zone, and they were closer to the atmospheric precipitation zone. This indicated that the chemical compositions of these two groundwater samples were affected by both rock weathering and atmospheric precipitation. Compared to rock weathering, atmospheric precipitation contributed more to the evolution of chemical compositions of these samples. Stable isotope analysis suggested that all groundwater in this study area mainly originated from atmospheric precipitation. In addition, field investigation found that sample GW11 and GW054 (outcropped from mountain) were close to the recharge area of groundwater, which led to a shorter residence time of groundwater runoff. Thus, the influence of rock weathering was relatively weaker for sample GW11 and GW054.

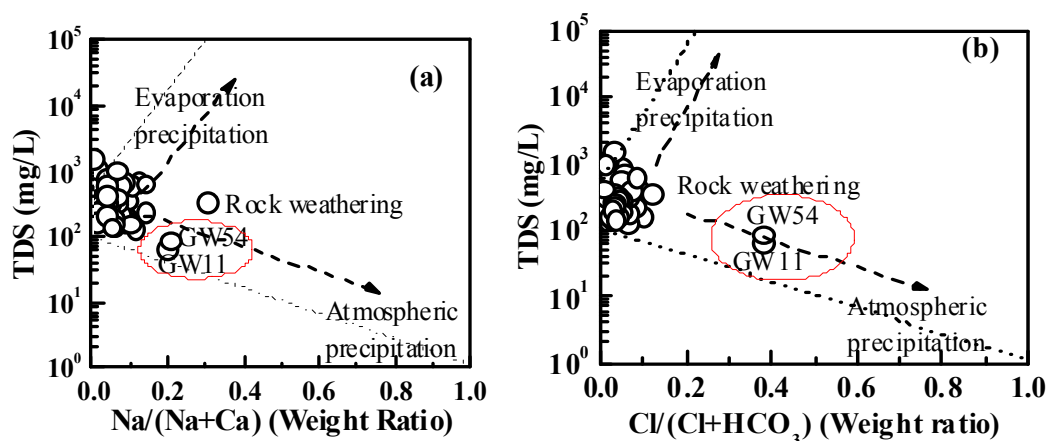
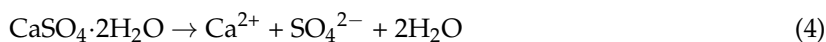
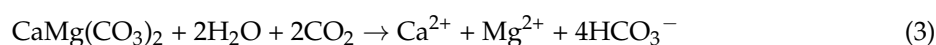


Figure 5. Gibbs diagrams for groundwater samples in the study area, (a) TDS versus $\text{Na}/(\text{Na} + \text{Ca})$, (b) TDS versus $\text{Cl}/(\text{Cl} + \text{HCO}_3)$.

5.1.1. Carbonate and Gypsum Dissolution

The analysis of groundwater chemistry demonstrated that Ca^{2+} , Mg^{2+} , HCO_3^- and SO_4^{2-} are the dominant ions in groundwater. The dissolution of carbonates (such as calcite and dolomite) and gypsum in karst aquifers generally provide these major ions in groundwater. The dissolution of calcite, dolomite, and gypsum can be expressed as follows:



According to Equations (2) and (3), the dissolution of calcite and dolomite would release equally charged amounts of Ca^{2+} and HCO_3^- , $(\text{Ca}^{2+} + \text{Mg}^{2+})$ and HCO_3^- , respectively. Namely, the equivalent charge ratio of Ca^{2+} and HCO_3^- , $(\text{Ca}^{2+} + \text{Mg}^{2+})$ and HCO_3^- should be equal 1:1. If the dissolution of calcite was the sole source of Ca^{2+} and HCO_3^- in groundwater, the ratio of Ca^{2+} and HCO_3^- in meq/L should be close to 1:1. Similarly, if the Ca^{2+} , Mg^{2+} , and HCO_3^- were only from the dissolution of dolomite, all of groundwater samples should be plotted along the 1:1 line of $(\text{Ca}^{2+} + \text{Mg}^{2+})$ and HCO_3^- . Theoretically, if the ratio of Ca^{2+} and HCO_3^- in meq/L were in the range of 1:1 to 1:2, the dissolution of the two carbonate minerals may have occurred simultaneously. In this study, almost all of the groundwater samples were plotted above the 1:1 line of $(\text{Ca}^{2+} + \text{Mg}^{2+})$ and HCO_3^- (Figure 6b), indicating that the dissolution of dolomite was not the sole source of Ca^{2+} , Mg^{2+} , and HCO_3^- in groundwater. In addition, some groundwater samples were distributed between the 1:1 and 1:2 lines of Ca^{2+} and HCO_3^- , meaning that the dissolution of calcite and dolomite was the major source of Ca^{2+} and HCO_3^- for these samples. Moreover, the derivation of several samples from the 1:1 line of Ca^{2+} and HCO_3^- (Figure 6a), suggested that another source should be accountable for the extra Ca^{2+} , such as the dissolution of gypsum minerals, and cation exchange between Ca^{2+} and Na^+ . The dissolution of gypsum would lead to more Ca^{2+} release to groundwater (Equation (4)). As shown in Figure 6c, the ratio of Ca^{2+} and SO_4^{2-} was greater than 1, indicated that the dissolution of gypsum was one of the sources of Ca^{2+} in groundwater. In order to determine the contribution of the dissolution of carbonate and gypsum minerals to groundwater chemistry, the ratios of $(\text{Ca}^{2+} + \text{Mg}^{2+})$ and $(\text{HCO}_3^- + \text{SO}_4^{2-})$ were also calculated and listed in Figure 6d. Previous studies suggested that if the samples distributed along the 1:1 line, the dissolution of carbonates and gypsum would be the sole source of Ca^{2+} , Mg^{2+} , HCO_3^- and SO_4^{2-} . As shown in Figure 6d, all samples spread on the 1:1 line of $(\text{Ca}^{2+} + \text{Mg}^{2+})$ and $(\text{HCO}_3^- + \text{SO}_4^{2-})$, meaning the crucial role of the dissolution of carbonates

and gypsum to groundwater chemistry. Furthermore, the SI indicated that most groundwater samples were saturated or nearly saturated with respect to calcite, except for some bedrock fissure groundwater samples. Therefore, the dissolution of calcite is relative weaker within this study area. On the contrary, almost all of groundwater samples were under-saturated with respect to dolomite, and the SI values of gypsum verified that gypsum was under-saturated in the aquifer. Thus, the dissolution of dolomite and gypsum may make significant contributions to the Ca^{2+} , Mg^{2+} , HCO_3^- and SO_4^{2-} in groundwater.

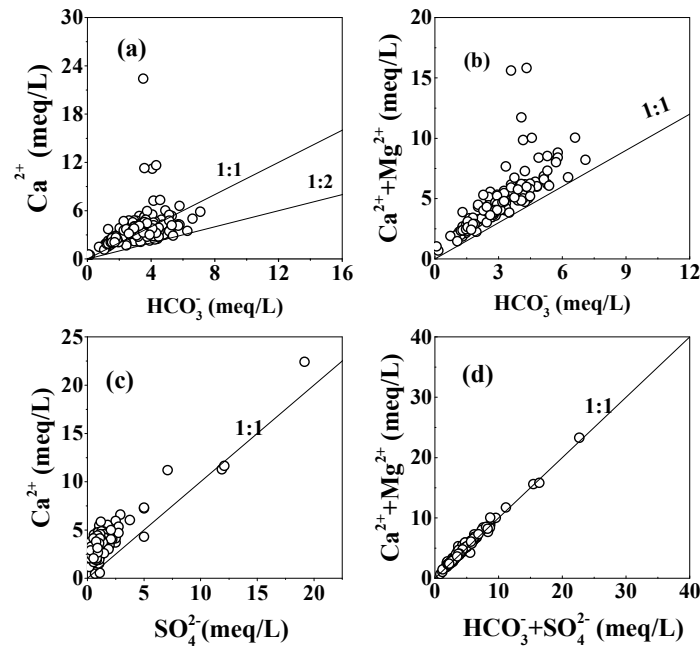
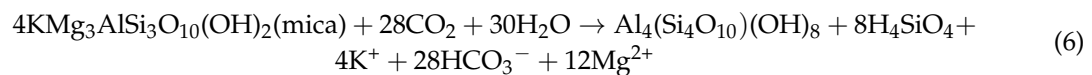
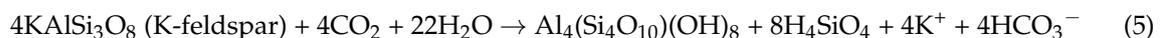


Figure 6. Relationships among major ions in groundwater samples. (a) Ca^{2+} versus HCO_3^- , (b) $(\text{Ca}^{2+} + \text{Mg}^{2+})$ versus HCO_3^- , (c) Ca^{2+} versus SO_4^{2-} , (d) $(\text{Ca}^{2+} + \text{Mg}^{2+})$ versus $(\text{HCO}_3^- + \text{SO}_4^{2-})$.

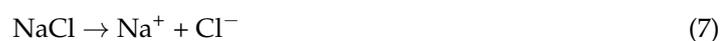
5.1.2. K-feldspar and Mica Minerals Dissolution

Besides carbonate rocks, clastic rocks are also observed in the study area. In addition, K-feldspar and mica are the principal minerals in clastic rocks. Therefore, the dissolution of K-feldspar and mica may contribute to K^+ , Mg^{2+} , and HCO_3^- in groundwater, which could be described in the following equations [48]:



5.1.3. Halite Minerals Dissolution

The results of PCA showed that PC4 was of great loading to Na^+ . The dissolution of halite was one of the important sources of Na^+ and Cl^- in groundwater. It can be described in the following equation:



If the dissolution of halite was the sole source of Na^+ and Cl^- in the aquifer, the ratio of Na^+ and Cl^- should be close to 1:1. The linear relationship between Na^+ and Cl^- suggested that the dissolution of halite was an important source of Na^+ and Cl^- in the groundwater (Figure 7). However, it found

that most of the groundwater samples were deviated from the 1:1 line of Na^+ and Cl^- . This indicated that Na^+ and Cl^- in groundwater not only originated from the dissolution of halite, but other sources such as cation exchange and human activities could elevate or decrease the concentration of Na^+ or Cl^- in groundwater. Furthermore, the SI values of halite for all groundwater were less than 0, meaning that the groundwater samples were under-saturated with respect to halite. Therefore, the dissolution of halite may take place in the aquifer in the study area.

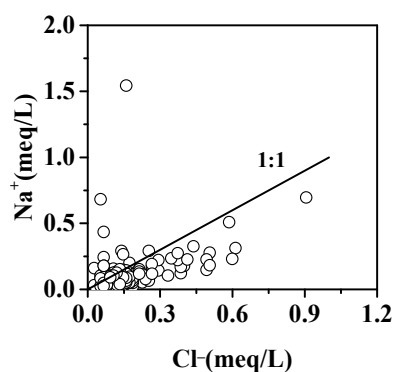


Figure 7. Plots of Na^+ and Cl^- in groundwater samples.

5.2. Cation Exchange

Cation exchange is an important hydrochemical process that has significant influence on the evolution of hydrochemical characteristics of groundwater [49]. The ratio of $[(\text{Ca}^{2+} + \text{Mg}^{2+}) - (\text{SO}_4^{2-} + \text{HCO}_3^-)]$ and $(\text{Na}^+ - \text{Cl}^-)$ is usually applied to evaluate the role of cation exchange taking place in the aquifer [46,50]. As shown in Figure 8a, the ratios of $[(\text{Ca}^{2+} + \text{Mg}^{2+}) - (\text{SO}_4^{2-} + \text{HCO}_3^-)] / (\text{Na}^+ - \text{Cl}^-)$ for most groundwater samples were close to 1:1, which indicated that cation exchange is a significant factor affecting the hydrochemical composition of groundwater [38]. The cation exchange can be quantified by the Chloro-Alkaline indices (CAI) [49]. CAI-I is defined as the ratio of $[\text{Cl}^- - (\text{Na}^+ + \text{K}^+)] / \text{Cl}^-$ (in meq/L). A positive value of CAI-I indicates cation exchange between Na^+ and K^+ in the groundwater with Ca^{2+} and Mg^{2+} in the aquifer medium, while a negative value of CAI indicates cation exchange taking place between Ca^{2+} and Mg^{2+} in the groundwater and Na^+ and K^+ in the aquifer medium. In this study, the values of CAI-I for about 34% groundwater samples were less than zero, indicating that Na^+ was released to groundwater from the aquifer medium through cation exchange. Other samples with CAI-I values greater than zero exhibited a reverse process (Figure 8b).

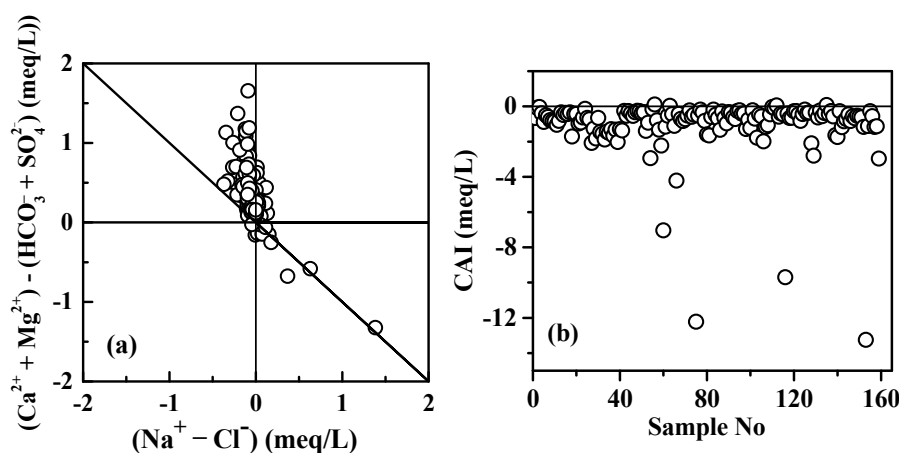


Figure 8. (a) Relationships between $[(\text{Ca}^{2+} + \text{Mg}^{2+}) - (\text{SO}_4^{2-} + \text{HCO}_3^-)]$ and $[(\text{Na}^+ - \text{Cl}^-)]$ in groundwater samples, (b) Chloro-Alkaline indices (CAI) of groundwater samples.

5.3. Anthropogenic Activities

Previous studies have demonstrated that anthropogenic activities such as use of chemical fertilizer, irrigation, waste disposal, and wastewater effluents may have effects on the chemical composition of groundwater [25,28,44]. In this study, the results of PCA also revealed that human activities could influence the hydrochemistry of groundwater. It has found that the concentration of NO_3^- was high in a small quantity of groundwater samples, and they mainly occurred around agricultural and urban areas, probably originating from sewage and intensive agricultural practices. The relationships between NO_3^- and other physiochemical parameters could be used to explain the impacts of anthropogenic activities on groundwater quality. The correlation analysis showed that there was good correlation between NO_3^- and Cl^- (the correlation coefficient was 0.54). In addition, both NO_3^- and Cl^- have high loading with PC3. The results indicated that NO_3^- and Cl^- derived from similar sources and supported the anthropogenic origin of contaminant. As mentioned above, the molar equivalent concentration of Cl^- was greater than that of Na^+ concentration in most of groundwater samples (Figure 7), the excessive Cl^- in groundwater may be explained by the infiltration of domestic wastewater and livestock, etc. Moreover, Bijie is a traditional agricultural zone and chemical fertilizer widely used in this region. The leaching of chemical fertilizer could lead to the increase of Na^+ in the groundwater, and thus the ratio of Na^+/Cl^- was greater than 1 in a few groundwater samples. Besides, it is worth noting that coal was in abundance in the study area. Extensive mining activity could significantly affect the hydrogeochemical characteristics of groundwater. In the present study, high concentration of SO_4^{2-} was found in some groundwater samples, and these samples were mainly distributed around the coalfield.

6. Conclusions

Shallow groundwater is an indispensable water resource of drinking and irrigation water in Bijie city, Guizhou Province. In this study, the hydrochemical incorporated SI and PCA were used to assess the evolution of groundwater in this typical karst zone. The chemical analysis showed that Ca^{2+} , Mg^{2+} , HCO_3^- and SO_4^{2-} were the dominant ions in almost all of the groundwater samples. The hydrochemical types of groundwater in this region were complex, and the main groundwater types were $\text{HCO}_3\text{-Ca}$, $\text{HCO}_3\text{-Ca-Mg}$, and $\text{HCO}_3\text{-SO}_4\text{-Ca}$. The results of SI calculations showed that most of the groundwater samples were nearly saturated or super-saturated with regard to calcite. Almost all of the groundwater samples were under-saturated with respect to dolomite, and gypsum and halite were under-saturated in all groundwater. Thus, the dissolution of dolomite, gypsum and halite may take place in the aquifer in the study area.

The PCA results combined with chemical analysis suggested that the hydrogeochemical characteristics of groundwater in the study area were mainly controlled by rock weathering such as the dissolution of calcite, dolomite, gypsum, and halite minerals, cation exchange between Ca^{2+} (Mg^{2+}) and Na^+ , and anthropogenic activities including sewage, intensive agricultural practices and extensive mining activity. This study revealed the dominant processes governing the hydrogeochemical characteristic of groundwater. The results would provide important insights into the local governments and then make an effective policy for groundwater utilization.

Acknowledgments: This study was supported by the Research Funds from National Nature Science Foundation (No: 41502245), and the China Geological Survey (Nos: 12120114030301 and DD20160286). We would like to thank the two anonymous reviewers and the editor for their constructive comments and suggestions on this manuscript.

Author Contributions: Jianfei Yuan had the original idea for the study, and performed the data analysis and drafted the manuscript. Guoshi Deng, Yeqi Tang, and Pengyue Li had collected the samples in field. Fen Xu reviewed and revised the manuscript, and made helpful suggestion.

Conflicts of Interest: The authors declare no conflict of interest.

References

1. Pu, T.; He, Y.; Zhang, T.; Wu, J.; Zhu, G.; Chang, L. Isotopic and geochemical evolution of ground and river waters in a karst dominated geological setting: A case study from Lijiang basin, South-Asia monsoon region. *Appl. Geochem.* **2013**, *33*, 199–212. [[CrossRef](#)]
2. Adinolfi Falcone, R.; Falgiani, A.; Parisse, B.; Petitta, M.; Spizzico, M.; Tallini, M. Chemical and isotopic ($\delta^{18}\text{O}\%$, $\delta^2\text{H}\%$, $\delta^{13}\text{C}\%$, ^{222}Rn) multi-tracing for groundwater conceptual model of carbonate aquifer (Gran Sasso INFN underground laboratory—Central Italy). *J. Hydrol.* **2008**, *357*, 368–388. [[CrossRef](#)]
3. Barberá, J.A.; Andreo, B. Hydrogeological processes in a fluviokarstic area inferred from the analysis of natural hydrogeochemical tracers. The case study of eastern Serranía de Ronda (S Spain). *J. Hydrol.* **2015**, *523*, 500–514.
4. Bhat, N.A.; Jeelani, G.; Bhat, M.Y. Hydrogeochemical assessment of groundwater in karst environments, Bringi watershed, Kashmir Himalayas, India. *Curr. Sci.* **2014**, *106*, 1000–1007.
5. Calijuri, M.L.; do Couto, d.E.A.; Santiago, d.A.F.; Camargo, d.R.A.; e Silva, M.D.F.M. Evaluation of the Influence of Natural and Anthropogenic Processes on Water Quality in Karstic Region. *Water Air Soil Poll.* **2012**, *223*, 2157–2168. [[CrossRef](#)]
6. López-Chicano, M.; Bouamama, M.; Vallejos, A.; Pulido-Bosch, A. Factors which determine the hydrogeochemical behaviour of karstic springs. A case study from the Betic Cordilleras, Spain. *Appl. Geochem.* **2001**, *16*, 1179–1192. [[CrossRef](#)]
7. Han, Y.; Wang, G.C.; Cravotta, C.A., III; Hu, W.Y.; Bian, Y.Y.; Zhang, Z.W.; Liu, Y.Y. Hydrogeochemical evolution of Ordovician limestone groundwater in Yanzhou, North China. *Hydrol. Process.* **2012**, *27*, 2247–2257. [[CrossRef](#)]
8. Jiang, Y.; Zhang, C.; Yuan, D.; Zhang, G.; He, R. Impact of land use change on groundwater quality in a typical karst watershed of southwest China: A case study of the Xiaojiang watershed, Yunnan Province. *Hydrogeol. J.* **2008**, *16*, 727–735. [[CrossRef](#)]
9. Lang, Y.-C.; Liu, C.-Q.; Zhao, Z.-Q.; Li, S.-L.; Han, G.-L. Geochemistry of surface and ground water in Guiyang, China: Water/rock interaction and pollution in a karst hydrological system. *Appl. Geochem.* **2006**, *21*, 887–903. [[CrossRef](#)]
10. Re, V.; Sacchi, E.; Mas-Pla, J.; Menció, A.; El Amrani, N. Identifying the effects of human pressure on groundwater quality to support water management strategies in coastal regions: A multi-tracer and statistical approach (Bou-Areg region, Morocco). *Sci. Total Environ.* **2014**, *500–501*, 211–223. [[CrossRef](#)] [[PubMed](#)]
11. Sun, Z.; Ma, R.; Wang, Y.; Ma, T.; Liu, Y. Using isotopic, hydrogeochemical-tracer and temperature data to characterize recharge and flow paths in a complex karst groundwater flow system in northern China. *Hydrogeol. J.* **2016**, *24*, 1393–1412. [[CrossRef](#)]
12. Wu, P.; Tang, C.; Zhu, L.; Liu, C.; Cha, X.; Tao, X. Hydrogeochemical characteristics of surface water and groundwater in the karst basin, southwest China. *Hydrol. Process.* **2009**, *23*, 2012–2022. [[CrossRef](#)]
13. Cloutier, V.; Lefebvre, R.; Therrien, R.; Savard, M.M. Multivariate statistical analysis of geochemical data as indicative of the hydrogeochemical evolution of groundwater in a sedimentary rock aquifer system. *J. Hydrol.* **2008**, *353*, 294–313. [[CrossRef](#)]
14. Galazoulas, E.; Petalas, C.; Tsihrantzis, V. Evaluation of multivariate statistical methods for the identification of groundwater facies, in a multilayered coastal aquifer. *Adv. Res. Aquat. Environ.* **2011**, *1*, 315–322.
15. Love, D.; Hallbauer, D.; Amos, A.; Hranova, R. Factor analysis as a tool in groundwater quality management: two southern African case studies. *Phys. Chem. Earth Pt. A/B/C* **2004**, *29*, 1135–1143. [[CrossRef](#)]
16. Menció, A.; Folch, A.; Mas-Pla, J. Identifying key parameters to differentiate groundwater flow systems using multifactorial analysis. *J. Hydrol.* **2012**, *472–473*, 301–313. [[CrossRef](#)]
17. Blake, S.; Henry, T.; Murray, J.; Flood, R.; Muller, M.R.; Jones, A.G.; Rath, V. Compositional multivariate statistical analysis of thermal groundwater provenance: A hydrogeochemical case study from Ireland. *Appl. Geochem.* **2016**, *75*, 171–188. [[CrossRef](#)]
18. Cortes, J.E.; Muñoz, L.F.; Gonzalez, C.A.; Niño, J.E.; Polo, A.; Suspes, A.; Siachoque, S.C.; Hernández, A.; Trujillo, H. Hydrogeochemistry of the formation waters in the San Francisco field, UMV basin, Colombia-A multivariate statistical approach. *J. Hydrol.* **2016**, *539*, 113–124. [[CrossRef](#)]
19. Davis, J.C. *Statistics and Data Analysis in Geology*, 3rd ed.; John Wiley & Sons: New Jersey, NJ, USA, 2002.

20. Hadj Ammar, F.; Chkir, N.; Zouari, K.; Hamelin, B.; Deschamps, P.; Aigoun, A. Hydro-geochemical processes in the Complexe Terminal aquifer of southern Tunisia: An integrated investigation based on geochemical and multivariate statistical methods. *J. Afr. Earth Sci.* **2014**, *100*, 81–95. [[CrossRef](#)]
21. Helstrup, T.; Jørgensen, N.; Banoeng-Yakubo, B. Investigation of hydrochemical characteristics of groundwater from the Cretaceous-Eocene limestone aquifer in southern Ghana and southern Togo using hierarchical cluster analysis. *Hydrogeol. J.* **2007**, *15*, 977–989. [[CrossRef](#)]
22. Jiang, Y.; Guo, H.; Jia, Y.; Cao, Y.; Hu, C. Principal component analysis and hierarchical cluster analyses of arsenic groundwater geochemistry in the Hetao basin, Inner Mongolia. *Chem. Erde-Geochem.* **2015**, *75*, 197–205. [[CrossRef](#)]
23. Koh, D.-C.; Chae, G.-T.; Ryu, J.-S.; Lee, S.-G.; Ko, K.-S. Occurrence and mobility of major and trace elements in groundwater from pristine volcanic aquifers in Jeju Island, Korea. *Appl. Geochem.* **2016**, *65*, 87–102. [[CrossRef](#)]
24. Moore, P.J.; Martin, J.B.; Sreaton, E.J. Geochemical and statistical evidence of recharge, mixing, and controls on spring discharge in an eogenetic karst aquifer. *J. Hydrol.* **2009**, *376*, 443–455. [[CrossRef](#)]
25. Omo-Irabor, O.O.; Olobaniyi, S.B.; Oduyemi, K.; Akunna, J. Surface and groundwater water quality assessment using multivariate analytical methods: A case study of the Western Niger Delta, Nigeria. *Phys. Chem. Earth, Pt. A/B/C* **2008**, *33*, 666–673. [[CrossRef](#)]
26. Salifu, A.; Petrusevski, B.; Ghebremichael, K.; Buamah, R.; Amy, G. Multivariate statistical analysis for fluoride occurrence in groundwater in the Northern region of Ghana. *J. Contam. Hydrol.* **2012**, *140–141*, 34–44. [[CrossRef](#)] [[PubMed](#)]
27. Voutsis, N.; Kelepertzis, E.; Tziritis, E.; Kelepertsis, A. Assessing the hydrogeochemistry of groundwaters in ophiolite areas of Euboea Island, Greece, using multivariate statistical methods. *J. Geochem. Explor.* **2015**, *159*, 79–92. [[CrossRef](#)]
28. Zghibi, A.; Merzougui, A.; Zouhri, L.; Tarhouni, J. Understanding groundwater chemistry using multivariate statistics techniques to the study of contamination in the Korba unconfined aquifer system of Cap-Bon (North-east of Tunisia). *J. Afr. Earth Sci.* **2014**, *89*, 1–15. [[CrossRef](#)]
29. Owen, D.D.R.; Cox, M.E. Hydrochemical evolution within a large alluvial groundwater resource overlying a shallow coal seam gas reservoir. *Sci. Total Environ.* **2015**, *523*, 233–252. [[CrossRef](#)] [[PubMed](#)]
30. Deng, G.; Tang, Y.; Li, P.; Yuan, J.; Liu, X.; Li, F. *Investigation Reports of 1:50,000 Hydrogeology and Environmental Geology Survey in the Wumeng Mountain*; Chengdu Center, China Geological Survey: Chengdu, China, 2015. (In Chinese)
31. Appelo, C.A.J.; Postma, D. *Geochemistry, Groundwater, and Pollution*; Balkema: Rotterdam, The Netherlands, 1996.
32. Epstein, S.; Mayeda, K. Variation of ^{18}O content of waters from natural sources. *Geochim. Cosmochim. Acta.* **1953**, *4*, 213–224. [[CrossRef](#)]
33. Coleman, M.L.; Shepherd, T.J.; Durham, J.J.; Rouse, J.E.; Moore, G.R. Reduction of water with zinc for hydrogen isotope analysis. *Anal. Chem.* **1982**, *54*, 993–995.
34. Parkhurst, D.L.; Appelo, C.A.J. *User's Guide to PHREEQC (version 2): A Computer Program for Speciation, Batch-reaction, One-dimensional Transport, and Inverse Geochemical Calculations*; Water-resources Investigations Report 99–4259; US Geological Survey, Earth Science Information Center, Open-File Reports Section: Denver, CO, USA, 1999.
35. Kim, J.-H.; Kim, R.-H.; Lee, J.; Cheong, T.-J.; Yum, B.-W.; Chang, H.-W. Multivariate statistical analysis to identify the major factors governing groundwater quality in the coastal area of Kimje, South Korea. *Hydrol. Process.* **2005**, *19*, 1261–1276. [[CrossRef](#)]
36. Kaiser, H.F. The Application of Electronic Computers to Factor Analysis. *Educ. Psychol. Meas.* **1960**, *20*, 141–151. [[CrossRef](#)]
37. Statistic IBM S. *IBM SPSS STATISTIC Program*, version 19; IBM Corporation: Armonk, NY, USA, 2011.
38. Li, P.-Y.; Wu, J.-H.; Qian, H. Hydrochemical appraisal of groundwater quality for drinking and irrigation purposes and the major influencing factors: a case study in and around Hua County, China. *Arab. J. Geosci.* **2016**, *9*, 1–17. [[CrossRef](#)]
39. World Health Organization (WHO). *Guidelines for Drinking Water Quality*, 3rd ed.; World Health Organization (WHO): Geneva, Switzerland, 2008.
40. Yuan, J. Hydrogeochemistry of the geothermal systems in coastal areas of Guangdong Province, south China. *Wuhan: China Univ. Geosci.* **2013**, *74–78*. (In Chinese)

41. Liu, W.; Wang, S.; Luo, W. The response of epikarst spring to precipitation and its implications in karst peak-cluster region of Libo Country, Guizhou Province, China. *Geochimica* **2011**, *40*, 487–496. (In Chinese)
42. Craig, H. Isotopic Variations in Meteoric Waters. *Science* **1961**, *133*, 1702–1703. [[CrossRef](#)] [[PubMed](#)]
43. Yang, P.; Yuan, D.; Yuan, W.; Kuang, Y.; Jia, P.; He, Q. Formations of groundwater hydrogeochemistry in a karst system during storm events as revealed by PCA. *Chinese. Sci. Bull.* **2010**, *55*, 788–797. (In Chinese) [[CrossRef](#)]
44. Yang, P.; Yuan, D.; Ye, X.; Xie, S.; Chen, X.; Liu, Z. Sources and migration path of chemical compositions in a karst groundwater system during rainfall events. *Chinese. Sci. Bull.* **2013**, *58*, 1755–1763. (In Chinese) [[CrossRef](#)]
45. Chen, K.; Jiao, J.J.; Huang, J.; Huang, R. Multivariate statistical evaluation of trace elements in groundwater in a coastal area in Shenzhen, China. *Environ. Pollut.* **2007**, *147*, 771–780. [[CrossRef](#)] [[PubMed](#)]
46. Huang, G.; Sun, J.; Zhang, Y.; Chen, Z.; Liu, F. Impact of anthropogenic and natural processes on the evolution of groundwater chemistry in a rapidly urbanized coastal area, South China. *Sci. Total Environ.* **2013**, *463–464*, 209–221. [[CrossRef](#)] [[PubMed](#)]
47. Gibbs, R.J. Mechanisms controlling world water chemistry. *Science* **1970**, *170*, 1088–1090. [[CrossRef](#)] [[PubMed](#)]
48. Zhang, G.; Deng, W.; He, Y.; Ramsis, S. Hydrochemical characteristics and evolution laws of groundwater in Songnen Plain, Northeast China. *Adv. Water Sci.* **2006**, *17*, 20–28. (In Chinese)
49. Charfi, S.; Zouari, K.; Feki, S.; Mami, E. Study of variation in groundwater quality in a coastal aquifer in north-eastern Tunisia using multivariate factor analysis. *Quatern. Int.* **2013**, *302*, 199–209. [[CrossRef](#)]
50. Wang, H.; Jiang, X.-W.; Wan, L.; Han, G.; Guo, H. Hydrogeochemical characterization of groundwater flow systems in the discharge area of a river basin. *J. Hydrol.* **2015**, *527*, 433–441. [[CrossRef](#)]



© 2017 by the authors. Licensee MDPI, Basel, Switzerland. This article is an open access article distributed under the terms and conditions of the Creative Commons Attribution (CC BY) license (<http://creativecommons.org/licenses/by/4.0/>).